Inorganic Chemistry

Article

pubs.acs.org/IC

Doping the Alkali Atom: An Effective Strategy to Improve the Electronic and Nonlinear Optical Properties of the Inorganic $Al_{12}N_{12}$ Nanocage

Min Niu,[†] Guangtao Yu,*[,†] Guanghui Yang,[‡] Wei Chen,*[,†] Xingang Zhao,[†] and Xuri Huang*[,†]

[†]The State Key Laboratory of Theoretical and Computational Chemistry, Institute of Theoretical Chemistry, Jilin University, Changchun 130023, People's Republic of China

[‡]Jilin Provincial Institute of Education, Changchun 130022, People's Republic of China

Supporting Information

ABSTRACT: Under ab initio computations, several new inorganic electride compounds with high stability, M@x-$Al_{12}N_{12}$ (M = Li, Na, and K; x = b_{66}, b_{64}, and r_6), were achieved for the first time by doping the alkali metal atom M on the fullerene-like $Al_{12}N_{12}$ nanocage, where the alkali atom is located over the Al−N bond (b_{66}/b_{64} site) or six-membered ring (r_6 site). It is revealed that independent of the doping position and atomic number, doping the alkali atom can significantly narrow the wide gap between the highest occupied molecular orbital (HOMO) and the lowest unoccupied molecular orbital (LUMO) ($E_{H\text{-}L}$ = 6.12 eV) of the pure $Al_{12}N_{12}$ nanocage in the range of 0.49−0.71 eV, and these doped AlN nanocages can exhibit the intriguing n-type characteristic, where a high energy level containing the excess electron is introduced as the new HOMO orbital in the original gap of pure $Al_{12}N_{12}$. Further, the diffuse excess electron also brings these doped AlN nanostructures the considerable first hyperpolarizabilities (β_0), which are 1.09 × 10^4 au for Li@b_{66}-$Al_{12}N_{12}$, 1.10 × 10^4, 1.62 × 10^4, 7.58 × 10^4 au for M@b_{64}-$Al_{12}N_{12}$ (M = Li, Na, and K), and 8.89 × 10^5, 1.36 × 10^5, 5.48 × 10^4 au for M@r_6-$Al_{12}N_{12}$ (M = Li, Na, and K), respectively. Clearly, doping the heavier Na/K atom over the Al−N bond can get the larger β_0 value, while the reverse trend can be observed for the series with the alkali atom over the six-membered ring, where doping the lighter Li atom can achieve the larger β_0 value. These fascinating findings will be advantageous for promoting the potential applications of the inorganic AlN-based nanosystems in the new type of electronic nanodevices and high-performance nonlinear optical (NLO) materials.

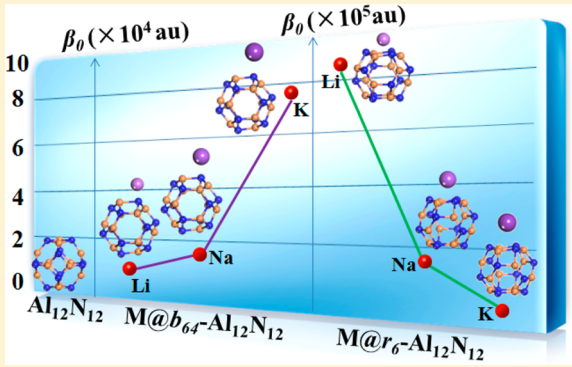

1. INTRODUCTION

In the past several decades, the design of novel materials with excellent nonlinear optical (NLO) properties has aroused great interest in experimental and theoretical fields, in view of the potential application in optical and electro-optical devices.[1−15] To date, some promising species with large NLO response have been considered as outstanding candidates to design new type of high-performance NLO materials,[2−15] for example, the inorganic NLO crystals with noncentrosymmetry,[2,3] the organic conjugated systems with donor-π bridge-acceptor framework,[4−7] the metal−ligand structures,[8−12] X-type chiral π-conjugated oligomers,[13] and octupolar molecules.[14,15]

Besides, the recent theoretical investigations[16−25] revealed that the systems containing the diffuse excess electron, such as, electrides and alkalides, can also exhibit considerably large first hyperpolarizability (β_0), where the diffuse excess electron plays a decisive role in increasing their β_0 values. Naturally, introducing the excess electron can be viewed as an effective approach to improve the NLO properties for different kinds of systems. For example, by incorporating the alkali metal atom M into organic calix[4]pyrrole, the obtained organometallic compounds, Li@calix[4]pyrrole[19] and Li^+(calix[4]pyrrole)M^- (M = Li, Na, and K),[20] can exhibit considerable β_0 values in the range of 7.33 × 10^3−2.45 × 10^4 au, almost 20−60 times larger than that of the undoped calix[4]pyrrole (only 390 au), where the outer s valence electron of the alkali atom M is pushed out to form the diffuse excess electron under the action of the lone pairs of N atoms of calix[4]pyrrole. Also, after doping the alkali Li atom, the deficient-electron $B_{10}H_{14}$ basket can present the β_0 value as large as 2.31 × 10^4 au, in which the s valence electron of the alkali Li atom is pulled to produce the diffuse excess electron[24] owing to the electron-withdrawing characteristic of $B_{10}H_{14}$. Moreover, very recently, we investigated the alkali metal atom interacting with a series of the π-conjugated aromatic rings (e.g., benzene, pyrrole, and thiophene)[25] and found that under the action of the π electron cloud of these aromatic rings, the s valence electron of the alkali metal atom

Received: September 9, 2013
Published: December 10, 2013

   dx.doi.org/10.1021/ic4022917 | *Inorg. Chem.* 2014, 53, 349−358

can be pushed out to produce the diffuse excess electron, resulting in the considerable β_0 value. This is advantageous for introducing the excess electron in the related systems with a π-conjugated aromatic ring to improve their NLO properties, such as in the attractive carbon nanomaterials and biomolecules.[25]

Obviously, the strategy of introducing diffuse excess electrons has been successfully proposed to design new type of high-performance NLO materials based on molecules, even extending to carbon nanostructures.[16−25] Motivated by these fascinating cases, in this work, we intend to improve the NLO response of inorganic nanostructures by means of introducing the excess electron. As the typical noncarbon hollow fullerene-like structures, the III−V group compounds are found to be an important source of nanoscale materials for their direct band gaps affording optical and electro-optical properties.[26−34] Lots of efforts have been directed toward the III−V fullerene-like nanostructures theoretically and experimentally,[35−41] particularly AlN nanocages, as one of the most important members, because of the fascinating physical and chemical properties (e.g., high thermal conductivity and chemical stability) endowing them with many potential applications in nanoscience.[42−44]

On the basis of ab initio calculation, it is revealed that in the large $(AlN)_n$ (n = 2−41) family, the $Al_{12}N_{12}$ cage is the most stable nanostructure energetically and thus it can be considered as an ideal inorganic fullerene-like candidate,[45] which has recently aroused researchers' extensive interest.[46−50] For example, the pure $Al_{12}N_{12}$ cage can exhibit an outstanding hydrogen storage capability[46] with a gravimetric density of hydrogen of 4.7 wt %, and doping Ni atoms on the $Al_{12}N_{12}$ cage can further increase the corresponding gravimetric density of hydrogen up to 6.8 wt %,[47] even surpassing the 2010 DOE target of 6 wt %. Also, it is predicted that the $Al_{12}N_{12}$ nanocage can act as the potential NO sensor device because of the high electronic sensitivity toward the adsorption of the NO molecule.[48] Besides, Beheshtian et al. found that the fluorination can change the inorganic $Al_{12}N_{12}$ nanocage from an intrinsic semiconductor to the intriguing p-type one, where the original wide gap between the highest occupied molecular orbital (HOMO) and the lowest unoccupied molecular orbital (LUMO) can be dramatically decreased.[49] Similarly, the wide HOMO−LUMO gap of the pure $Al_{12}N_{12}$ cage can be also narrowed by doping the transition metal (TM) on the $Al_{12}N_{12}$ cage to form thermodynamically stable TM@$(AlN)_{12}$ (TM = Ti, Mn, Fe, Co, and Ni) compounds.[50] These can be assumed to be particularly important for promoting the applications of inorganic AlN-based nanomaterials in the future nanoscale electronic devices.

Clearly, some efforts have been made for the $Al_{12}N_{12}$ nanocages, which are mainly focused on effectively tuning the electronic property,[49,50] besides some other studies about the potential applications in hydrogen storage[46,47] and as gas sensor.[48] To our best knowledge, however, the correlative reports on the NLO property (e.g., the first hyperpolarizability) are rather scarce.

In this work, we performed comprehensive ab initio computations to investigate how the doping alkali atom will effectively improve not only the electronic but also the NLO properties of the inorganic AlN-based nanostructures by sampling the $Al_{12}N_{12}$ nanocage with high stability, where the alkali atom M (M = Li, Na, and K) is doped on the surface of $Al_{12}N_{12}$ (denoted as M@$Al_{12}N_{12}$). It is worth mentioning that some cases of the alkali metal atom adsorbing on other organic (e.g., C_{60} fullerene)[51−54] or inorganic (e.g., $B_{36}N_{36}$ and B_{80})[55−57] nanocages have been extensively investigated as the potential materials of hydrogen storage.[51−57] Besides, the low-dimensional nanosystems doped by the alkali metal atom/cluster, such as, C_{60} fullerene,[58,59] carbon nanotube,[60−62] and inorganic BN nanotube,[63,64] have been studied for their geometrical structures and corresponding NLO properties.

Specifically, in this study, we will mainly address the following issues: (1) Can the excess electron be produced as the alkali atom M interacting with the $Al_{12}N_{12}$ nanocage? (2) If the diffuse excess electron is introduced, can it cause large first hyperpolarizability for these doped inorganic $Al_{12}N_{12}$ nanocages? (3) Can the alkali atom effectively bind with the $Al_{12}N_{12}$ moiety with considerable binding energies? (4) Are the first hyperpolarizability (β_0) values of M@$Al_{12}N_{12}$ (M = Li, Na, and K) dependent on the alkali metal atomic number and doping position? (5) How will doping alkali metal atom affect the electronic property of the pure $Al_{12}N_{12}$ nanocage with the wide HOMO−LUMO gap? By resolving them, this work can provide some new valuable insights into the design of multifunctional AlN-based nanodevices exhibiting the excellent electronic property as well as considerable NLO response. Our computed results revealed that doping alkali atom M on the $Al_{12}N_{12}$ nanocage can not only effectively narrow the wide HOMO−LUMO gap (from 6.12 eV to a range of 0.49−0.71 eV), endowing these doping structures with the intriguing n-type characteristic, but also significantly increase the first hyperpolarizabilities in the range of 1.09×10^4−8.89×10^5 au. Note that this work is the first successful attempt to devise novel multifunctional inorganic AlN-based nanostructures by doping the alkali atom in theory, which can promote their potential applications in electronic devices and high-performance NLO materials.

2. COMPUTATIONAL DETAILS

When a system is in the weak and homogeneous electric field, its energy can be written as[65,66]

$$E = E^0 - \mu_\alpha F_\alpha - \frac{1}{2}\alpha_{\alpha\beta}F_\alpha F_\beta - \frac{1}{6}\beta_{\alpha\beta\gamma}F_\alpha F_\beta F_\gamma - \ldots \quad (1)$$

Here, E^0 is the molecular total energy without the electric field, and F_α is the electric field component along α direction; μ_α, $\alpha_{\alpha\beta}$, and $\beta_{\alpha\beta\gamma}$ are the dipole, the polarizability, and the first hyperpolarizability, respectively.

The mean polarizability and first hyperpolarizability are denoted as

$$\alpha = \frac{1}{3}(\alpha_{xx} + \alpha_{yy} + \alpha_{zz}) \quad (2)$$

$$\beta_0 = (\beta_x^2 + \beta_y^2 + \beta_z^2)^{1/2} \quad (3)$$

where

$$\beta_i = \frac{3}{5}(\beta_{iii} + \beta_{ijj} + \beta_{ikk}) \quad i, j, k = x, y, z \quad (4)$$

The geometric structures with all real frequencies are obtained at the B3LYP/6-31+G(d) level, where the doublet state is considered for all the doped systems. Here, we also performed a computational test to investigate the effects of different methods and basis sets on the optimized geometrical structures by sampling Li@b_{64}-$Al_{12}N_{12}$, in which the alkali Li atom is located over the Al−N bond fused between the one six- and one four-membered rings (b_{64} site) of the AlN nanocage. It is found that the geometrical parameters obtained at the B3LYP/6-31+G(d) level can be close to the corresponding ones from the other methods (Supporting Information, Table S1) or basis sets

dx.doi.org/10.1021/ic4022917 | Inorg. Chem. 2014, 53, 349−358

(Supporting Information, Table S2), indicating that the B3LYP method and 6-31+G(d) basis set should be reliable for geometry optimization in this study. More detailed discussions have been provided at the Section (I) in the Supporting Information.

Further, the second-order Møller–Plesset perturbation (MP2) method, accompanied by the 6-31+G(d) basis set, is chosen to calculate the polarizability and first hyperpolarizability (β_0) of all the studied systems, considering that the computed results from the MP2 method can be close to those obtained from the more sophisticated correlation methods (for example, the quadratic configuration interaction with single and double excitations (QCISD)[17]). Furthermore, the employed 6-31+G(d) basis set is also appropriate to compute β_0 values of systems in this study, as confirmed by the related computational test at the Section (I) in the Supporting Information, Table S3. For all the calculations of hyperpolarizability, the magnitude of the applied electric field is set as 0.001 au. In this work, we considered the spin contamination of all the computations on the geometrical optimization and NLO response, and found that the corresponding $\langle S^2 \rangle$ values are in the range of 0.752–0.756, which are very close to the value 0.750 for the pure doublet state, indicating that the spin contamination is negligible and the computational results are reliable.

Moreover, the time-dependent density functional theory (TD-DFT) calculations were performed at the M06-2X/6-31+G(d) level to achieve the crucial excited states of the related structures, and the differences of their dipole moments between the ground state and crucial excited state were evaluated by employing the configuration interaction singles (CIS) method with the same basis set. The B3LYP/6-311++G(3df, 3pd) method is used for the calculation of the natural bond orbital (NBO) charges of the systems.

To understand the stability of these doped $Al_{12}N_{12}$ cages with alkali metal atom M, their corresponding binding energies (E_b) are evaluated according to the following equation:

$$E_b = E(Al_{12}N_{12}) + E(M) - E(M@Al_{12}N_{12})$$

where the $E(Al_{12}N_{12})$, $E(M)$, and $E(M@Al_{12}N_{12})$ are the total energies with the zero-point vibrational energies (ZPVE) correction for the undoped $Al_{12}N_{12}$ molecule, the alkali atom M, and the corresponding doped system $M@Al_{12}N_{12}$, respectively.

All of the calculations were carried out by using the GAUSSIAN 09 program package.[67]

3. RESULTS AND DISCUSSION

3.1. Geometrical Characteristics of M@*x*-$Al_{12}N_{12}$ (M = Li, Na, and K; *x* = b_{66}, b_{64}, and r_6). Initially, we performed a detailed investigation on the Li atom interacting with the inorganic $Al_{12}N_{12}$ nanocage by considering all of possible doping sites, namely, over the aluminum atom (denoted as Al site), nitrogen atom (N site), the Al–N bond fused between two six-membered rings (b_{66} site) or one six- and one four-membered rings (b_{64} site), and the center of the six- (r_6 site) or the four-membered ring (r_4 site). Among them, three geometrical structures with all real frequencies are achieved, and they are named as Li@b_{66}-$Al_{12}N_{12}$, Li@b_{64}-$Al_{12}N_{12}$, and Li@r_6-$Al_{12}N_{12}$, respectively, where the Li atom is located over the corresponding b_{66}, b_{64}, and r_6 sites. Also, four additional structures doped by heavier alkali atom M (M = Na and K), namely, Na@b_{64}-$Al_{12}N_{12}$, K@b_{64}-$Al_{12}N_{12}$, Na@r_6-$Al_{12}N_{12}$, and K@r_6-$Al_{12}N_{12}$, are obtained to investigate the effect of the alkali atomic number on the corresponding electronic (Section 3.2) and NLO properties (Section 3.3) of the doped systems. Note that we only choose the b_{64} site as a representative to investigate the influence of doping the heavier alkali M atom at the Al–N bond site, since doping Li atom at b_{64} site of $Al_{12}N_{12}$ (Li@b_{64}-$Al_{12}N_{12}$) can lead to almost same electronic and NLO properties as at the b_{66} site (Li@b_{66}-$Al_{12}N_{12}$), as will be discussed in the Sections 3.2 and 3.3. Moreover, for the purpose of comparison, the pure $Al_{12}N_{12}$ compound with T_h symmetry is also considered (Figure 1a), in which the Al–N bond lengths corresponding to the b_{66} and b_{64} sites are 1.793 and 1.858 Å, respectively, in good agreement with the earlier reports.[36,48]

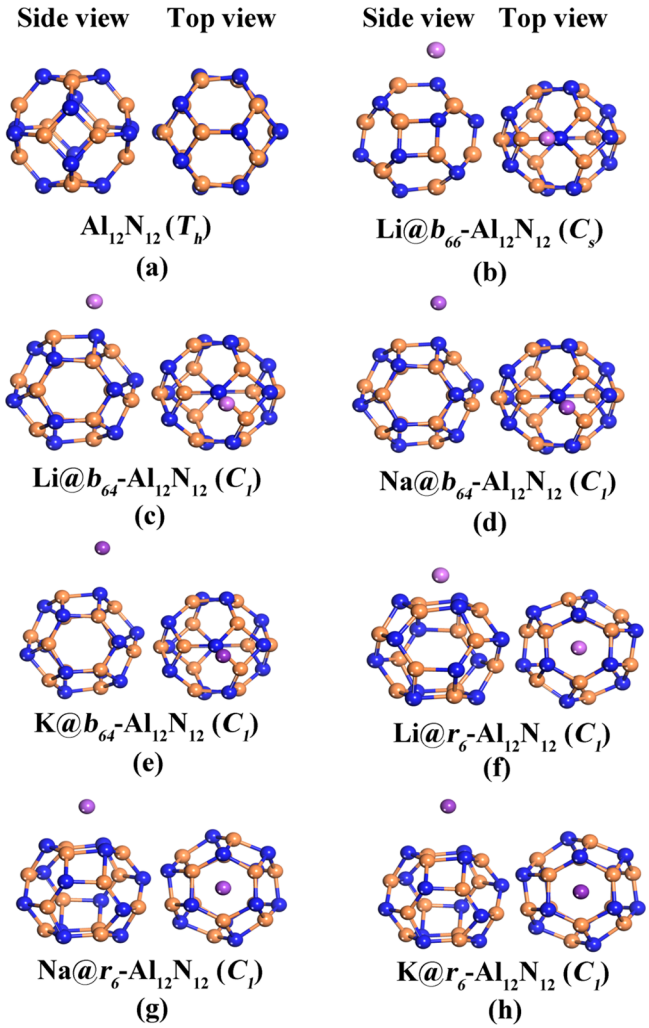

Figure 1. Side and top views of the optimized structures including the undoped $Al_{12}N_{12}$ and doped M@*x*-$Al_{12}N_{12}$ (*x* = b_{66}, b_{64}, and r_6, M = Li, Na, and K). The aurantium and blue balls represent Al and N atoms, respectively.

As shown in Figure 1, except for Li@b_{66}-$Al_{12}N_{12}$ with C_s symmetry, all of the remaining doped systems M@b_{64}-$Al_{12}N_{12}$ and M@r_6-$Al_{12}N_{12}$ (M = Li, Na, and K) belong to the C_1 point group. Compared with the undoped inorganic $Al_{12}N_{12}$ cage, it is found that doping alkali atom M can elongate the Al–N bond length at the corresponding doping position in M@*x*-$Al_{12}N_{12}$. Specifically, when the alkali atom M interacts with the b_{66}/b_{64} site, the corresponding doped Al–N bond (R_{b66}/R_{b64}) can be significantly lengthened by 0.100 Å (Table 1), where the vertical distances between the M atom and this Al–N bond (denoted as $d_{M\text{-bond}}$) are 1.854 Å for Li@b_{66}-$Al_{12}N_{12}$, and 1.849, 2.272, 2.656 Å for M = Li, Na, and K in the M@b_{64}-$Al_{12}N_{12}$ series, respectively, exhibiting the increasing trend as the M atomic number increases. The similar enhanced trend of the vertical distances between the M atom and the center of r_6 ring (denoted as $d_{M\text{-ring}}$) can be also observed in the M@r_6-$Al_{12}N_{12}$

dx.doi.org/10.1021/ic4022917 | Inorg. Chem. 2014, 53, 349–358

Table 1. HOMO-LUMO Gap ($E_{H\text{-}L}$), the Binding Energy (E_b), the NBO Charge (q) on Alkali Atom M, the Symmetry, and the Main Geometrical Parameters of the $Al_{12}N_{12}$ and M@x-$Al_{12}N_{12}$ (x = b_{66}, b_{64}, and r_6, M = Li, Na, and K) Molecules[a]

			M@b_{64}-$Al_{12}N_{12}$			M@r_6-$Al_{12}N_{12}$		
properties	$Al_{12}N_{12}$	Li@b_{66}-$Al_{12}N_{12}$	Li	Na	K	Li	Na	K
$E_{H\text{-}L}$ (eV)	6.12	0.68	0.70	0.71	0.63	0.55	0.49	0.66
E_b (kcal/mol)		33.2	33.5	19.4	19.2	21.1	11.7	15.6
q		0.618	0.620	0.531	0.607	0.615	0.535	0.634
$d_{M\text{-}bond}$[b] (Å)		1.854	1.849	2.272	2.656			
$d_{M\text{-}ring}$[c] (Å)						1.555	2.294	2.770
R_{b64}[d] (Å)	1.858		2.021 (0.163)	1.960 (0.102)	1.953 (0.095)	1.893 (0.035)	1.881 (0.023)	1.880 (0.022)
R_{b66}[d] (Å)	1.793	1.923 (0.130)				1.817 (0.024)	1.809 (0.016)	1.811 (0.018)
symmetry	T_h	C_s	C_1	C_1	C_1	C_1	C_1	C_1

[a]The value in the parentheses means the change of corresponding Al−N bond in the doped systems, compared with that in the pure $Al_{12}N_{12}$. [b]The vertical distance between the M atom and its doped Al−N bond fused between two six-membered rings (b_{66} bond) or one six- and one four-membered rings (b_{64} bond). [c]The vertical distance between the M atom and the center of its doped six-membered ring (r_6). [d]The bond length of corresponding doped b_{64} or b_{66} bond.

series, namely, 1.555 Å (M = Li) < 2.294 Å (Na) < 2.770 Å (K), yet all of the Al−N bonds (R_{b66}/R_{b64}) involved in the six-membered ring interacting with the M atom are only slightly elongated in the range of 0.016−0.035 Å, in contrast to the significant extension of the Al−N bond directly doped with the alkali atom in M@b_{64}-$Al_{12}N_{12}$ series. Moreover, the doping alkali atom can also cause the occurrence of charge transfer from the alkali M atom to the inorganic $Al_{12}N_{12}$ cage, and the alkali atoms can exhibit the positive charge in the range of 0.531−0.634e in these doped systems Li@b_{66}-$Al_{12}N_{12}$, M@b_{64}-$Al_{12}N_{12}$, and M@r_6-$Al_{12}N_{12}$ (M = Li, Na, and K), as found by the NBO computed results (Table 1).

Furthermore, we calculated the binding energies (E_b) to understand the stability of these combined compounds by doping the alkali atom on the inorganic $Al_{12}N_{12}$ cage. The computed results showed that all of the seven structures exhibit remarkably large binding energies (E_b) of 33.2, 33.5, 19.4, 19.2, 21.1, 11.7, and 15.6 kcal/mol for Li@b_{66}-$Al_{12}N_{12}$, Li@b_{64}-$Al_{12}N_{12}$, Na@b_{64}-$Al_{12}N_{12}$, K@b_{64}-$Al_{12}N_{12}$, Li@r_6-$Al_{12}N_{12}$, Na@r_6-$Al_{12}N_{12}$, and K@r_6-$Al_{12}N_{12}$, respectively, much larger than 10 kcal/mol, indicating that independent of the doping position and alkali atomic number, these M@x-$Al_{12}N_{12}$ species can possess considerable structural stability, particularly for the Li@x-$Al_{12}N_{12}$ (x = b_{66}, b_{64}, and r_6) series (E_b > 20 kcal/mol). Here, the infrared adsorption and Raman spectra for these Li-doped AlN systems with higher stability have been provided to assist their future experimental measurement, as shown in the Section (II) of Supporting Information.

3.2. Electronic Properties of M@x-$Al_{12}N_{12}$ (M = Li, Na, and K; x = b_{66}, b_{64}, and r_6). It is well-known that the pure inorganic AlN nanocages can exhibit intrinsic insulator properties, hindering their potential applications in the nanoscale electronic devices. For example, as found by our computed results, the large energy gap (denoted as $E_{H\text{-}L}$) of about 6.12 eV between the highest occupied (HOMO) and lowest unoccupied molecular orbitals (LUMO) can be observed for the $Al_{12}N_{12}$ cage. In this work, we take the $Al_{12}N_{12}$ cage as an example, and intend to understand whether doping alkali metal atom can effectively decrease the large $E_{H\text{-}L}$ value of these inorganic AlN nanocages.

From Table 1, our computational results found that doping the alkali atom M (M = Li, Na, and K) can remarkably decrease the $E_{H\text{-}L}$ value of the pure inorganic $Al_{12}N_{12}$ cage, and endow the doped systems M@x-$Al_{12}N_{12}$ (M = Li, Na, and K; x = b_{66}, b_{64}, and r_6) with a considerably small $E_{H\text{-}L}$ value in the range of 0.49−0.71 eV, only as large as 10% of the $E_{H\text{-}L}$ value (6.12 eV) for the undoped $Al_{12}N_{12}$ cage.

Why can doping the alkali atom M effectively narrow the large energy gap of the $Al_{12}N_{12}$ cage? To understand this intriguing issue, we have plotted the total density of states (TDOS) and partial density of states (PDOS) of the undoped $Al_{12}N_{12}$ and doped M@x-$Al_{12}N_{12}$ series, respectively (Figure 2), where their corresponding frontier molecular orbitals (HOMO, HOMO-1, and LUMO) have been also pictured. By comparison, it is found that doping the alkali atom M can introduce a high energy level as the newly formed HOMO lying between the original HOMO (becoming HOMO-1 of doped systems) and LUMO of $Al_{12}N_{12}$ cage, which is responsible for the significant decrease of the considerable $E_{H\text{-}L}$ gap, transforming these doped M@x-$Al_{12}N_{12}$ structures into the n-type semiconductor. The computed DOS results revealed that the newly resulting HOMO level originates from not only the doping alkali atom M but also the doped part of the $Al_{12}N_{12}$ moiety (Figure 2). Further, from the HOMOs for these doped M@x-$Al_{12}N_{12}$ systems (Figure 2), we can uniformly find that under the action of the lone pairs of the N atoms, the outer s valence electron of the alkali atom M can be pushed out to become the diffuse excess electron, which can effectively heighten the newly formed HOMO energy level, resulting in the occurrence of a small $E_{H\text{-}L}$ value for these doped systems.

Obviously, doping alkali metal atoms can be a simple and effective approach to decrease the large $E_{H\text{-}L}$ gap of the inorganic AlN nanocages by introducing the diffuse excess electron to produce a high energy state as new HOMO, almost irrespective of the doping position and alkali atomic number. This can be considered as a new strategy to overcome the bottleneck of a wide HOMO−LUMO gap in the inorganic AlN nanostructures and endow them with a typical n-type semiconducting behavior, promoting their potential applications for future AlN-based nanoscale electronic devices.

3.3. Nonlinear Optical Properties of M@x-$Al_{12}N_{12}$ (M = Li, Na, and K; x = b_{66}, b_{64}, and r_6). *3.3.1. NLO Properties of Li@x-$Al_{12}N_{12}$ (x = b_{66}, b_{64}, and r_6).* Considering that the existence of the diffuse excess electron can usually cause the large NLO response, revealed by the previous studies,[16−25] it is highly expected that these M@x-$Al_{12}N_{12}$ (M = Li, Na, and K; x = b_{66}, b_{64}, and r_6) species with high stability can exhibit a considerable first hyperpolarizability (β_0). Here, we initially performed computations on the polarizability and static first hyperpolarizability of the doped $Al_{12}N_{12}$ systems (Li@x-

dx.doi.org/10.1021/ic4022917 | Inorg. Chem. 2014, 53, 349−358

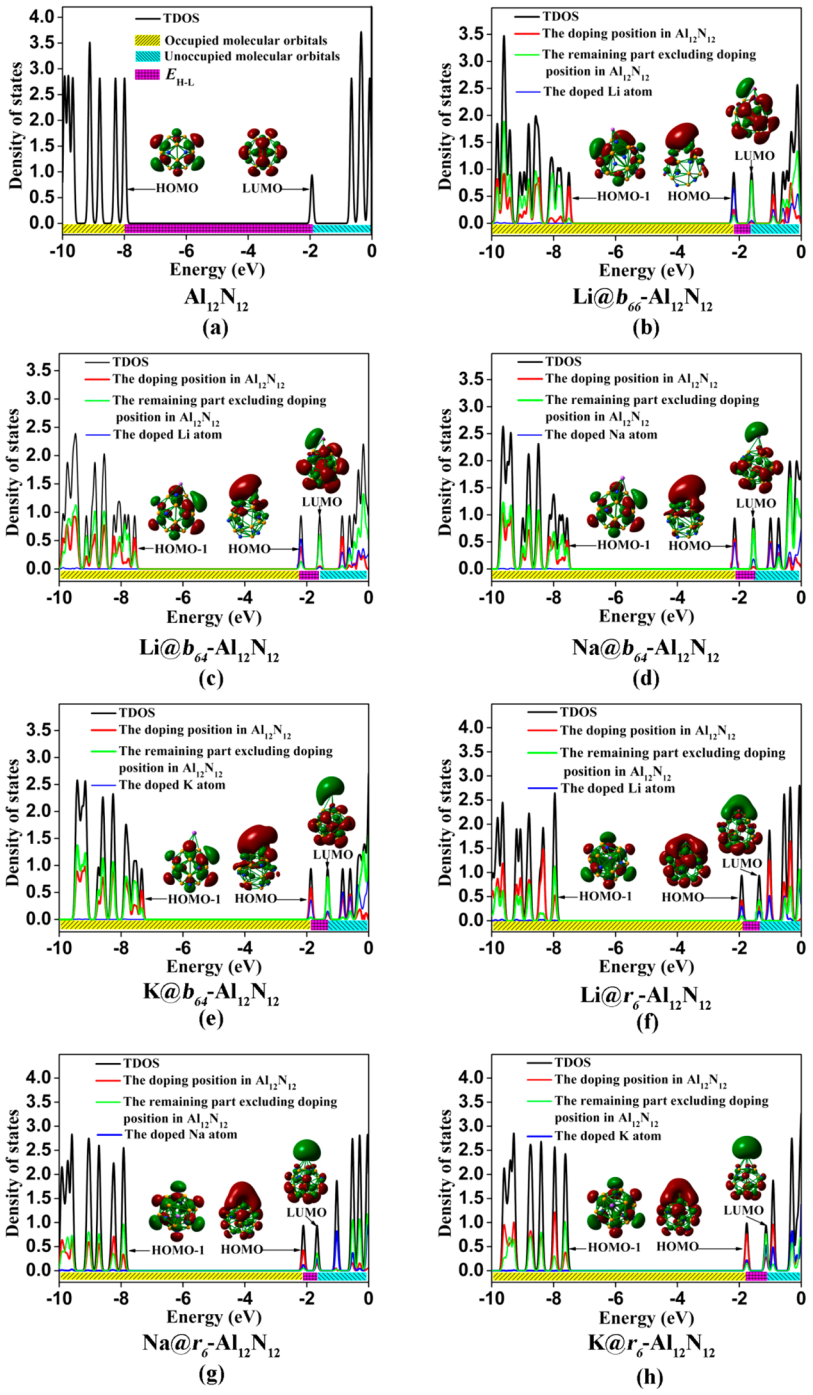

Figure 2. Total density of states (TDOS) and partial density of states (PDOS) of the undoped $Al_{12}N_{12}$ and doped M@x-$Al_{12}N_{12}$ (x = b_{66}, b_{64}, and r_6, M = Li, Na, and K) molecules derived from the ROM06-2X method. The corresponding frontier molecular orbitals are also shown as the insets.

$Al_{12}N_{12}$, x = b_{66}, b_{64}, and r_6) with alkali Li atom at different positions, to determine whether the doping alkali atom can effectively improve the NLO response of the inorganic AlN systems and how the doping position of alkali atom will affect the polarizability and first hyperpolarizability of the related systems.

Our computed results revealed that doping the alkali Li atom can somewhat change the polarizability of the undoped $Al_{12}N_{12}$ molecule (α = 308 au), that is, Li atom over the Al−N bond (b_{66} and b_{64}) can slightly increase the α value (379 au for Li@b_{66}-$Al_{12}N_{12}$ and Li@b_{64}-$Al_{12}N_{12}$), while the slight decreasing trend can be observed in Li@r_6-$Al_{12}N_{12}$ (269 au) with the Li atom over the six-membered ring (r_6 site). Different from the polarizability, doping the alkali Li atom can significantly enhance the first hyperpolarizability of the undoped $Al_{12}N_{12}$ molecule (β_0 = 0 au), and all of three doped Li@x-$Al_{12}N_{12}$ systems can uniformly exhibit considerable β_0 values up to 1.09×10^4, 1.10×10^4, and 8.89×10^5 au for x = b_{66}, b_{64}, and r_6 sites, respectively, where doping Li atom over the r_6 site can more effectively increase the β_0 value than over the b_{66} and b_{64} Al−N bonds (with almost equivalent β_0 value).

To understand why doping alkali Li atom and the different doping positions can produce this effect on the β_0 value, we may use the two-level expression:[68,69]

dx.doi.org/10.1021/ic4022917 | Inorg. Chem. 2014, 53, 349−358

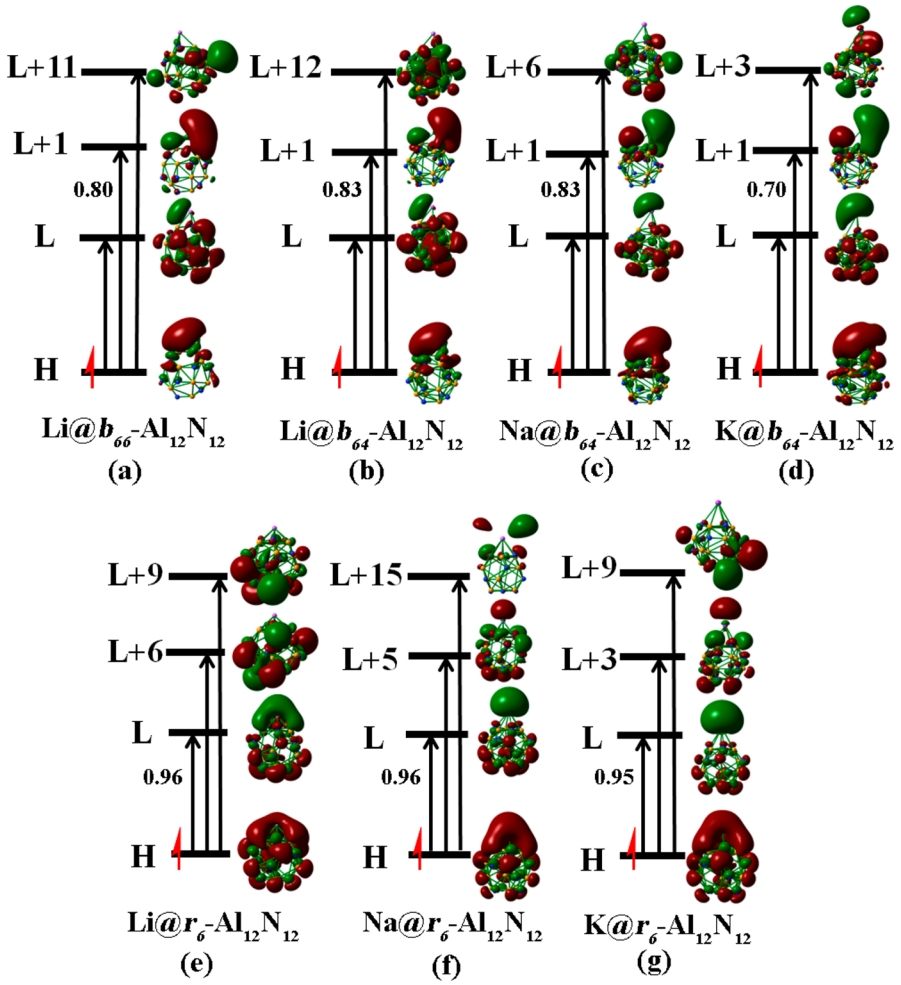

Figure 3. Crucial transition states of the Li@b_{66}-$Al_{12}N_{12}$, M@b_{64}-$Al_{12}N_{12}$, and M@r_6-$Al_{12}N_{12}$ (M = Li, Na, and K) molecules, where the largest component coefficient is marked.

$$\beta_0 \propto \Delta\mu \cdot f_0 / \Delta E^3$$

where ΔE, f_0, and $\Delta\mu$ are the crucial transition energy, the largest oscillator strength, and the difference of dipole moment between the ground state and the crucial excited state (the excited state with the largest oscillator strength), respectively.

The TD-DFT computations were performed to obtain the crucial excited states of the doped systems Li@x-$Al_{12}N_{12}$ (x = b_{66}, b_{64}, and r_6), as shown in Figures 3a, 3b and 3e, respectively. It is found that the electron involved in the crucial excited states of these species is uniformly from their respective HOMO orbital, in which under the action of lone pairs of N atoms in the $Al_{12}N_{12}$ moiety, the *2s* valence electron of the Li atom is pushed out to the highly diffuse *s* orbital to become the excess electron, and the resulting HOMO orbitals are mainly composed of the diffuse *s* orbitals of the Li atom. Accordingly, it is reasonable to expect that these Li@x-$Al_{12}N_{12}$ systems can display much smaller crucial transition energy ΔE than the undoped $Al_{12}N_{12}$ molecule, since the interaction between the diffuse excess electron and the Li core is greatly weakened, and it can usually be easily excited.

Indeed, as revealed by our computed results, in contrast to the undoped $Al_{12}N_{12}$ nanocage (as large as 5.83 eV), the ΔE values of the doped Li@x-$Al_{12}N_{12}$ systems can sharply decrease to 1.75, 1.76, and 1.21 eV for x = b_{66}, b_{64}, and r_6 sites, respectively. Such small ΔE values can result in the considerably large β_0 values in the Li@x-$Al_{12}N_{12}$ (x = b_{66}, b_{64}, and r_6) series because the third power of ΔE is inversely proportional to the β_0 value according to the two-level state model. Moreover, the larger β_0 value of doped Li@x-$Al_{12}N_{12}$ system with Li atom located over the r_6 site (8.89×10^5 au for Li@r_6-$Al_{12}N_{12}$) than over b_{66} and b_{64} bond sites (1.09×10^4 and 1.10×10^4 au for Li@b_{66}-$Al_{12}N_{12}$ and Li@b_{64}-$Al_{12}N_{12}$, respectively) can be also attributed to the much smaller ΔE value (1.21 eV) of the former than those of the latter two structures (1.75 and 1.76 eV, respectively). It is worth mentioning that the estimated β_0 values of all three doped Li@x-$Al_{12}N_{12}$ systems (410, 482, and 5933 au for x = b_{66}, b_{64}, and r_6, respectively), by considering the related parameters ΔE, f_0, and $\Delta\mu$ under two-level state model, can also exhibit a similar trend to the computed β_0 values (1.09×10^4, 1.10×10^4 and 8.89×10^5 au for x = b_{66}, b_{64}, and r_6, respectively), as shown in Figure 4.

Obviously, doping the alkali atom can be proposed to be a simple and effective strategy to enhance the first hyperpolarizability of the inorganic $Al_{12}N_{12}$ nanocage, where doping position can also play a crucial role in increasing the NLO response.

3.3.2. Monotonic Dependency of the First Hyperpolarizabilities of M@b_{64}-$Al_{12}N_{12}$ and M@r_6-$Al_{12}N_{12}$ (M = Li, Na, and K). On the basis that doping alkali Li atom can significantly improve the first hyperpolarizability of the inorganic $Al_{12}N_{12}$

dx.doi.org/10.1021/ic4022917 | *Inorg. Chem.* 2014, 53, 349−358

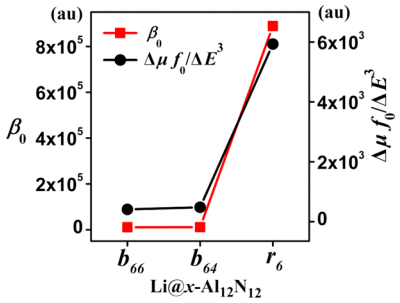

Figure 4. Effect of different doping position on the computational β_0 value and the corresponding estimated β_0 value by using the two-level model ($\Delta\mu{\cdot}f_0/\Delta E^3$) of Li@$x$-$Al_{12}N_{12}$ (x = b_{66}, b_{64}, and r_6).

nanocage, naturally, we further wonder how increasing alkali atomic number will affect the first hyperpolarizability of these doped $Al_{12}N_{12}$ systems. It is well-known that the ionization potential of alkali metal atoms M (M = Li, Na, and K) become lower along with increasing the atomic number, therefore, the *s* valence electron of heavier alkali atom is more easily pushed out to form the diffuse excess electron, and it is expected that doping heavier alkali metal atom can result in larger first hyperpolarizability. Indeed, in previous reports, the heavier alkali atom doping systems with the excess electron can usually exhibit the larger β_0 value, such as, M@Calix[4]pyrrole (M = Li, Na, and K),[19,70] and $M_2^{\bullet+}$ $TCNQ^{\bullet-}$ (M = Li, Na, and K).[71] Naturally, it is reasonable for us to anticipate that by means of doping heavier alkali atom Na/K can more effectively improve the NLO response of the inorganic $Al_{12}N_{12}$ cage in this study.

Initially, we investigated the effect of doping the heavier alkali atom M on the first hyperpolarizability of the doped $Al_{12}N_{12}$ structure with the M atom located over the Al−N bond by only sampling the b_{64} bond site, considering that Li@b_{64}-$Al_{12}N_{12}$ has almost the same α (∼ 379 au) and β_0 (∼ 1.10×10^4 au) values as Li@b_{66}-$Al_{12}N_{12}$ with Li atom doping the b_{66} site. Our computed results revealed that as increasing the alkali atomic number, α values can increase slightly for the M@b_{64}-$Al_{12}N_{12}$ series, namely, 379 au (M = Li) < 443 au (Na) < 517 au (K), as shown in the Table 2. In particular, a more significant trend of monotonic increase can be observed for the β_0 values of the M@b_{64}-$Al_{12}N_{12}$ series (Table 2), that is, 1.10×10^4 au (M = Li) < 1.62×10^4 au (Na) < 7.58×10^4 au (K). Clearly, the β_0 values of M@b_{64}-$Al_{12}N_{12}$ (M = Li, Na, and K) systems can be dependent on the alkali atomic number, and doping the heavier alkali atom Na/K at the Al−N bond site can cause the larger β_0 values of the doped systems, which can be mainly attributed to the gradually lower ionization potential along with increasing the atomic number, similar to the previous cases mentioned above.[19,70,71]

Subsequently, we also investigated the effect of doping the heavier alkali Na/K atom over the six-membered ring (r_6 site) on the polarizability and first hyperpolarizability of the M@r_6-$Al_{12}N_{12}$ series. Different from the case of the heavier alkali atom doping over the Al−N bond, the computed results revealed that compared with the light Li atom, introducing the heavier Na/K atom in M@r_6-$Al_{12}N_{12}$ can increase the α value, 269 au (M = Li) < 886 au (Na) < 1325 au (K), yet significantly decrease the β_0 value: 8.89×10^5 au > 1.36×10^5 au > 5.48×10^4 au for M = Li, Na, and K, respectively. Obviously, the entirely opposite trend of the β_0 values between M@r_6-$Al_{12}N_{12}$ and M@b_{64}-$Al_{12}N_{12}$ (M = Li, Na, and K) series can be observed, along with the change of coordination number of alkali M atom due to the different doping sites. It is worth mentioning that the similar situation on the decreasing trend of β_0 value with increasing alkali atom number for the M@r_6-$Al_{12}N_{12}$ series can also be observed in our recent investigation on the M@pyrrole (M = Li and Na) systems[25] with alkali Li/Na atom locating over the pyrrole ring, which can be mainly attributed to the fact that the geometric distance (d) between M and its doped aromatic ring, rather than the ionization potential of alkali atom M, plays a crucial role in impacting the β_0 value. Here, we also performed computations to investigate the curves of the β_0 for M@r_6-$Al_{12}N_{12}$ (M = Li, Na, and K) as a function of the vertical distance ($d_{\text{M-ring}}$) between M and the center of its doped six-membered ring. As shown in Supporting Information, Figure S3, for all of the M@r_6-$Al_{12}N_{12}$ systems, increasing the vertical distance $d_{\text{M-ring}}$ can result in the decrease of corresponding β_0 values. Additionally, to further confirm the crucial effect of $d_{\text{M-ring}}$, we also made a comparison between the β_0 values of the M@r_6-$Al_{12}N_{12}$ (M = Li, Na, and K) series with the alkali M atom located at the same $d_{\text{M-ring}}$ site on three curves. It can be found that, distinct from the decreasing β_0 order for the optimized M@r_6-$Al_{12}N_{12}$ structures, the corresponding β_0 values of the three structures at the each sampled site with the same $d_{\text{M-ring}}$ value can exhibit a totally reverse trend, that is, β_0 values increase with increase of the alkali atomic number (Supporting Information, Figure S3), just like most of previous

Table 2. Polarizability (α), the First Hyperpolarizability (β_0), the Transition Energy (ΔE), the Difference of Dipole Moment between the Ground State and the Crucial Excited State ($\Delta\mu$), the Largest Oscillator Strength (f_0), the Estimated β_0 Value under the Two-Level State ($\Delta\mu{\cdot}f_0/\Delta E^3$), and the Main Compositions of the Crucial Transition State (CT) of the Pure $Al_{12}N_{12}$ and M@x-$Al_{12}N_{12}$ (x = b_{66}, b_{64}, and r_6, M = Li, Na, and K) Molecules

			M@b_{64}-$Al_{12}N_{12}$			M@r_6-$Al_{12}N_{12}$		
properties	$Al_{12}N_{12}$	Li@b_{66}-$Al_{12}N_{12}$	Li	Na	K	Li	Na	K
α (au)	308	379	379	443	517	269	886	1325
β_0 (au)	0	1.09×10^4	1.10×10^4	1.62×10^4	7.58×10^4	8.89×10^5	1.36×10^5	5.48×10^4
ΔE (eV)	5.83	1.75	1.76	1.21	1.44	1.21	0.98	1.03
$\Delta\mu$ (au)	0	0.598	0.741	0.764	2.003	3.198	0.843	0.556
f_0	0.2209	0.1814	0.1749	0.2470	0.1929	0.1613	0.2809	0.2565
$\Delta\mu{\cdot}f_0/\Delta E^3$		410	482	2143	2617	5933	5103	2604
CT		H→L[a]	H→L	H→L	H→L	H→L	H→L	H→L
		H→L+1	H→L+1	H→L+1	H→L+1	H→L+6	H→L+5	H→L+3
		H→L+11	H→L+12	H→L+6	H→L+3	H→L+9	H→L+15	H→L+9

[a]H and L mean the highest occupied (HOMO) and lowest unoccupied molecular orbitals (LUMO), respectively.

dx.doi.org/10.1021/ic4022917 | *Inorg. Chem.* 2014, 53, 349−358

cases, where the ionization potential of alkali atom performs again a crucial role in determining β_0 value. Obviously, all of these can reflect that the vertical distance ($d_{M\text{-ring}}$) can dominate the trend of the β_0 values, which is responsible for the decrease of β_0 value in M@r_6-$Al_{12}N_{12}$ (M = Li, Na, and K) series with increasing the alkali atomic number.

Further, we also employed the two-level expression to understand the corresponding increasing/decreasing trend of the β_0 values of M@b_{64}-$Al_{12}N_{12}$ or M@r_6-$Al_{12}N_{12}$ (M = Li, Na, and K) series with the increase of alkali atomic number.

Initially, we performed the TD-DFT computations on M@b_{64}-$Al_{12}N_{12}$ (M = Na and K) systems, and the computed results revealed that employing the heavier atom Na/K (1.21/1.44 eV) can result in much smaller ΔE value than with the lighter Li atom (1.76 eV), which is responsible for the larger β_0 values achieved by doping the heavier alkali atom Na/K at the Al−N bond site. However, it can be easily found that the ΔE value is not an exclusive factor in determining the β_0 order between Na@b_{64}-$Al_{12}N_{12}$ and K@b_{64}-$Al_{12}N_{12}$ systems doped by heavier Na/K atom, in view of the ΔE value of the former (1.21 eV) slightly smaller than the latter (1.44 eV). Accordingly, we further considered the effect of the other two parameters (f_0 and $\Delta\mu$) in the two-level state model on the first hyperpolarizability for both of the heavier Na/K doping systems. It is found that the computed f_0 value (0.2470) of Na@b_{64}-$Al_{12}N_{12}$ is slightly larger than that (0.1929) of K@b_{64}-$Al_{12}N_{12}$. Therefore, by combining their ΔE and f_0 under the two-level state model, it is reasonable to expect that the $\Delta\mu$ value should be a decisive factor in dominating the larger β_0 value of K@b_{64}-$Al_{12}N_{12}$ (7.58×10^4 au) than Na@b_{64}-$Al_{12}N_{12}$ (1.62×10^4 au). Indeed, the computed $\Delta\mu$ value of K@b_{64}-$Al_{12}N_{12}$ is considerable, about 2.003 au, which is almost three times as large as that of the Na@b_{64}-$Al_{12}N_{12}$ (0.764 au). This is enough to overcome the negative effect from the ΔE and f_0 values on the β_0 order between Na@b_{64}-$Al_{12}N_{12}$ and K@b_{64}-$Al_{12}N_{12}$ systems, making their β_0 values monotonically increase with increasing alkali atomic number (Figure 5a).

Further, to understand the reason for the much larger $\Delta\mu$ value of the K-doped than of the Na-doped systems, we can go to trace the specific distribution of the electron cloud for the occupied and unoccupied molecular orbitals involved in the crucial excited states of both doped systems. As shown in Figure 3, the transition of HOMO→LUMO+1 is a dominant component (with the coefficient > 0.70) in the crucial excited states for Na@b_{64}-$Al_{12}N_{12}$ and K@b_{64}-$Al_{12}N_{12}$, where the electron cloud in their LUMO+1 orbital mainly centralizes on the alkali Na/K atom and presents almost the same distribution shape, while in their HOMO orbitals, except for the similar distribution on the Na/K atom, the electron cloud locating on the surface of the $Al_{12}N_{12}$ cage can become more and more toward the opposite direction of the M-doping site along with increasing the atomic number. This trend can be also reflected by their corresponding DOS results (Figures 2d and 2e): in the HOMO of Na@b_{64}-$Al_{12}N_{12}$, the component from the $Al_{12}N_{12}$ moiety (red line) is comparable to that from the alkali atom (blue line); whereas the corresponding former component becomes much larger than the latter one in the HOMO of K@b_{64}-$Al_{12}N_{12}$. Accordingly, when the transition of electron occurs from the HOMO to the LUMO+1 orbitals, the incremental transfer distance from the $Al_{12}N_{12}$ moiety to the alkali atom can result in the significant increase of the $\Delta\mu$ values with increasing the alkali atomic number, leading to the monotonic increasing trend of the β_0 values.

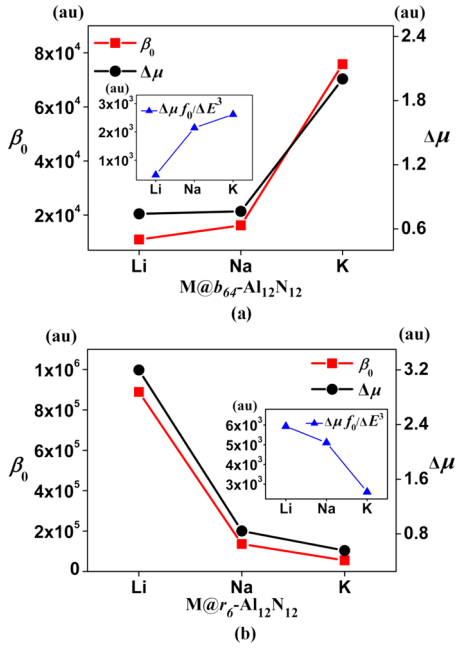

Figure 5. Relationship between the computational β_0 and $\Delta\mu$ of (a) M@b_{64}-$Al_{12}N_{12}$ and (b) M@r_6-$Al_{12}N_{12}$ (M = Li, Na, and K) as the alkali atomic number increases. The corresponding estimated β_0 values under the two-level expression ($\Delta\mu \cdot f_0/\Delta E^3$) are shown in the inset picture.

Subsequently, to understand the reason why employing heavier Na/K atom leads to the decrease of the β_0 value in the M@r_6-$Al_{12}N_{12}$ series, we computed three parameters ΔE, f_0, and $\Delta\mu$ invoked in the two-level expression. From Table 2, it is found that Na@r_6-$Al_{12}N_{12}$ (0.98 eV) and K@r_6-$Al_{12}N_{12}$ (1.03 eV) have almost the same ΔE value, both of which are smaller than that of Li@r_6-$Al_{12}N_{12}$ (1.21 eV). Moreover, the computed f_0 values of Na@r_6-$Al_{12}N_{12}$ (0.2809) and K@r_6-$Al_{12}N_{12}$ (0.2565) are also comparable, which are larger than that of Li@r_6-$Al_{12}N_{12}$ (0.1613). According to the two-level state model, therefore, it is clear that both ΔE and f_0 values are not the dominant factors in decreasing the β_0 values of the M@r_6-$Al_{12}N_{12}$ series (M = Li, Na, and K), indicating that the $\Delta\mu$ value should be a decisive factor in determining the much smaller β_0 value of the doped systems with the heavier Na/K atom than the light Li atom. This has been confirmed by our computed results: the computed $\Delta\mu$ values of Na@r_6-$Al_{12}N_{12}$ (0.843 au) and K@r_6-$Al_{12}N_{12}$ (0.556 au) are much smaller than that of Li@r_6-$Al_{12}N_{12}$ (3.198 au), which is consistent with the decreasing trend of the corresponding β_0 values (Figure 5b).

Further, to better understand the decrease of $\Delta\mu$ values resulted from doping the heavier Na/K atom, we also examined the HOMO and LUMO orbitals of the M@r_6-$Al_{12}N_{12}$ (M = Li, Na, and K) series, in view of the case that the transition of HOMO→LUMO can uniformly dominate their crucial excited states (with the coefficient > 0.95), as shown in Figure 3e−g. It can be found that the distribution of the electron cloud in all the correlative LUMO orbitals can present a relatively similar shape for the M@r_6-$Al_{12}N_{12}$ (M = Li, Na, and K) series, independent of the alkali atomic number. However, different from the LUMO case, compared with the approximatively average distribution of the electron cloud in the involved HOMO orbital of the Li@r_6-$Al_{12}N_{12}$, the electron cloud in the HOMOs of the parallel Na/K-doping $Al_{12}N_{12}$ cage can exhibit significant polar behavior, resulting in much larger dipole

dx.doi.org/10.1021/ic4022917 | Inorg. Chem. 2014, 53, 349−358

moment of the ground state than the corresponding Li case. This should be responsible for much smaller $\Delta\mu$ value of the doped $Al_{12}N_{12}$ system with the heavier Na/K atom than the light Li atom when the HOMO→LUMO transition occurs.

Moreover, we also estimated the β_0 values of the M@b_{64}-$Al_{12}N_{12}$ and M@r_6-$Al_{12}N_{12}$ series under the two-level state model by considering all three factors ΔE, $\Delta\mu$, and f_0. It is revealed that for both the series, the trend of the estimated β_0 values is consistent with their corresponding computed β_0 values. Specifically, the estimated β_0 values of M@b_{64}-$Al_{12}N_{12}$ (482 au (M = Li) < 2143 au (Na) < 2617 au (K)) can exhibit a similar monotonically increasing trend to that of their computed β_0 values (1.10×10^4 au (Li) < 1.62×10^4 au (Na) < 7.58×10^4 au (K)) (Figure 5a). Likewise, the estimated β_0 values of M@r_6-$Al_{12}N_{12}$ (5933 au (M = Li) > 5103 au (Na) > 2604 au (K)) can present a similar deceasing trend to the computed β_0 values (8.89×10^5 au (Li) > 1.36×10^5 au (Na) > 5.48×10^4 au (K)) (Figure 5b).

Obviously, dependent on the doping position, the alkali atomic number can cause distinctly different effects on the NLO responses of the doped $Al_{12}N_{12}$ systems, that is, employing heavier alkali Na/K atom can bring the larger first hyperpolarizability for the structure with the alkali atom locating over the Al−N bond, while doping the light Li atom is more effective to enhance the first hyperpolarizability of the structure with the alkali atom locating over the six-membered ring of the $Al_{12}N_{12}$ nanocage.

4. CONCLUSIONS

In this work, we proposed a new approach through doping alkali atom M to effectively improve the electronic and NLO properties of the inorganic $Al_{12}N_{12}$ nanosystem, by means of performing a detailed theoretical investigation on the M@x-$Al_{12}N_{12}$ (M = Li, Na, and K; x = b_{66}, b_{64}, and r_6) series. It is revealed that all of these new doped AlN nanocages can present the interesting n-type semiconducting behavior with a small energy gap ($E_{H\text{-}L}$) in the range of 0.49−0.71 eV, which can be attributed to the case that the doping alkali atom can produce a new high energy level involving the excess electron to serve as new HOMO in the original gap of $Al_{12}N_{12}$. Obviously, this is advantageous for overcoming the bottleneck that the inorganic $Al_{12}N_{12}$ nanocage is difficult in the application to electronic nanodevices owing to the considerably large $E_{H\text{-}L}$ (ca. 6.12 eV).

Further, doping alkali atom can also cause the considerably large first hyperpolarizability (β_0) in the range of 1.09×10^4−8.89×10^5 au for these new M@$Al_{12}N_{12}$ compounds, compared with that for the undoped $Al_{12}N_{12}$ nanocage. Specifically, when doping the alkali atom over the Al−N bond, employing the heavier Na/K atom is advantageous for achieving the larger β_0 value in the M@b_{64}-$Al_{12}N_{12}$ series, while doping the lighter Li atom over the six-membered ring site can more effectively increase the β_0 value of the M@r_6-$Al_{12}N_{12}$ series. Moreover, all of the doped $Al_{12}N_{12}$ nanostructures can exhibit high stability, as confirmed by their computed considerable binding energies with larger than 10 kcal/mol (E_b = 11.7−33.5 kcal/mol).

Undoubtedly, doping the alkali atom can effectively improve not only the electronic behavior but also the NLO properties of the inorganic $Al_{12}N_{12}$ nanocage, which will be advantageous for promoting the multifield applications of the inorganic AlN-based nanostructures in electronic nanodevices and high-performance NLO nanomaterials.

■ ASSOCIATED CONTENT

Supporting Information

(I) The effect of computational method and basis set on geometry optimization (Table S1 and Table S2), and basis set effect on the computed first hyperpolarizability (β_0) (Table S3); (II) the infrared absorption (IR) and Raman spectra of pure $Al_{12}N_{12}$ cage and Li@x-$Al_{12}N_{12}$ (x = b_{66}, b_{64}, and r_6) structures (Figure S1 and Figure S2); (III) the first hyperpolarizability (β_0) versus the vertical distance ($d_{M\text{-ring}}$) between the M atom and the center of its doped six-membered ring (r_6) for the M@r_6-$Al_{12}N_{12}$ (M = Li, Na, and K) series (Table S4 and Figure S3); (IV) the details of computations on the convergence criteria for geometry optimization (Table S5) and the SCF convergence criteria (Table S6), as well as the optimized coordinates of all the studied systems with input keywords. This material is available free of charge via the Internet at http://pubs.acs.org.

■ AUTHOR INFORMATION

Corresponding Authors

*E-mail: yugt@jlu.edu.cn (G.Y.).
*E-mail: xychwei@gmail.com (W.C.).
*E-mail: xurihuang09@gmail.com (X.H.).

Notes

The authors declare no competing financial interest.

■ ACKNOWLEDGMENTS

This work was supported in China by NSFC (21103065, 21373099, 21073075 and 21173097), National Basic Research Program of China (973 Program) (2012CB932800), the Ministry of Education of China (20110061120024 and 20100061110046), and Science and Technology Research Program of Higher Education of Jilin Province, China ([2011] No. 388). G.T.Y. and W.C. thank the equipment funds (450091105163 and 450091105164) from Jilin University. We acknowledge the High Performance Computing Center (HPCC) of Jilin University for supercomputer time.

■ REFERENCES

(1) Stahelin, M.; Burland, D. M.; Rice, J. E. *Chem. Phys. Lett.* **1992**, *191*, 245.
(2) Zhang, H. X.; Zhang, J.; Zheng, S. T.; Wang, G. M.; Yang, G. Y. *Inorg. Chem.* **2004**, *43*, 6148.
(3) Xu, X.; Hu, C. L.; Kong, F.; Zhang, J. H.; Mao, J. G.; Sun, J. L. *Inorg. Chem.* **2013**, *52*, 5831.
(4) Williams, D. J., Ed.; *Nonlinear Optical Properties of Organic Molecules and Polymeric Materials*; ACS Symposium Series 233; American Chemical Society: Washington, DC, 1984.
(5) Schulz, M.; Tretiak, S.; Chernyak, V.; Mukamel, S. *J. Am. Chem. Soc.* **2000**, *122*, 452.
(6) Priyadarshy, S.; Therien, M. J.; Beratan, D. N. *J. Am. Chem. Soc.* **1996**, *118*, 1504.
(7) Xiao, D. Q.; Bulat, F. A.; Yang, W. T.; Beratan, D. N. *Nano Lett.* **2008**, *8*, 2814.
(8) de la Torre, G.; Vaquez, P.; Agullo-Lopez, F.; Torres, T. *Chem. Rev.* **2004**, *104*, 3723.
(9) Liu, C. G.; Guan, W.; Song, P.; Yan, L. K.; Su, Z. M. *Inorg. Chem.* **2009**, *48*, 6548.
(10) Zhang, T. G.; Zhao, Y.; Asselberghs, I.; Persoons, A.; Clays, K.; Therien, M. T. *J. Am. Chem. Soc.* **2005**, *127*, 9710.
(11) Tancrez, N.; Feuvrie, C.; Ledoux, I.; Zyss, J.; Toupet, L.; Bozec, H. L.; Maury, O. *J. Am. Chem. Soc.* **2005**, *127*, 13474.
(12) Coe, B. J.; Fielden, J.; Foxon, S. P.; Asselberghs, I.; Clays, K.; Brunschwig, B. S. *Inorg. Chem.* **2010**, *49*, 10718.

(13) Cornelis, D.; Franz, E.; Asselberghs, I.; Clays, K.; Verbiest, T.; Koeckelberghs, G. *J. Am. Chem. Soc.* **2011**, *133*, 1317.
(14) Maury, O.; Viau, L.; Senechal, K.; Corre, B.; Guegan, J. P.; Renouard, T.; Ledoux, I.; Zyss, J.; Bozec, L. H. *Chem.—Eur. J.* **2004**, *10*, 4454.
(15) Lee, S. H.; Park, J. R.; Jeong, M. Y.; Kim, H. M.; Li, S. J.; Song, J.; Ham, S.; Jeon, S. J.; Cho, B. R. *ChemPhysChem* **2006**, *7*, 206.
(16) Chen, W.; Li, Z. R.; Wu, D.; Gu, F. L.; Hao, X. Y.; Wang, B. Q.; Li, R. J.; Sun, C. C. *J. Chem. Phys.* **2004**, *121*, 10489.
(17) Chen, W.; Li, Z. R.; Wu, D.; Li, R. Y.; Sun, C. C. *J. Phys. Chem. B* **2005**, *109*, 601.
(18) Chen, W.; Li, Z. R.; Wu, D.; Li, Y.; Sun, C. C. *J. Phys. Chem. A* **2005**, *109*, 2920.
(19) Chen, W.; Li, Z. R.; W, D.; Li, Y.; Sun, C. C.; Gu, F. L. *J. Am. Chem. Soc.* **2005**, *127*, 10977.
(20) Chen, W.; Li, Z. R.; Wu, D.; Li, Y.; Sun, C. C.; Gu, F. L.; Aoki, Y. *J. Am. Chem. Soc.* **2006**, *128*, 1072.
(21) Xu, H. L.; Li, Z. R.; Wu, D.; Wang, B. Q.; Li, Y.; Gu, F. L.; Aoki, Y. *J. Am. Chem. Soc.* **2007**, *129*, 2967.
(22) Wang, F. F.; Li, Z. R.; Wu, D.; Wang, B. Q.; Li, Y.; Li, Z. J.; Chen, W.; Yu, G. T.; Gu, F. L.; Aoki, Y. *J. Phys. Chem. B* **2008**, *112*, 1090.
(23) Li, Z. J.; Wang, F. F.; Li, Z. R.; Xu, H. L.; Huang, X. R.; Wu, D.; Chen, W.; Yu, G. T.; Gu, F. L.; Aoki, Y. *Phys. Chem. Chem. Phys.* **2009**, *11*, 402.
(24) Muhammad, S.; Xu, H. L.; Liao, Y.; Kan, Y. H.; Su, Z. M. *J. Am. Chem. Soc.* **2009**, *131*, 11833.
(25) Yu, G. T.; Huang, X. R.; Chen, W.; Sun, C. C. *J. Comput. Chem.* **2011**, *32*, 9.
(26) Strout, D. L. *J. Phys. Chem. A* **2000**, *104*, 3364.
(27) Wang, R. X.; Zhang, D. J.; Liu, C. B. *Chem. Phys. Lett.* **2005**, *411*, 333.
(28) Bertolus, M.; Finocchi, F.; Millié, P. *J. Chem. Phys.* **2004**, *120*, 9.
(29) Golberg, D.; Bando, Y.; Stéphan, O.; Kurashima, K. *Appl. Phys. Lett.* **1998**, *73*, 17.
(30) Stafström, S.; Hultman, L.; Hellgren, N. *Chem. Phys. Lett.* **2001**, *340*, 227.
(31) Fu, C. C.; Weissmann, M.; Machado, M.; Ordejón, P. *Phys. Rev. B* **2001**, *63*, 085411.
(32) Peyghan, A. A.; Pashangpour, M.; Bagheri, Z.; Kamfiroozi, M. *Phys. E* **2012**, *44*, 1436.
(33) Beheshtian, J.; Peyghan, A. A.; Bagheri, Z.; Kamfiroozi, M. *Struct. Chem.* **2012**, *23*, 1567.
(34) Beheshtian, J.; Bagheri, Z.; Kamfiroozi, M.; Ahmadi, A. *Microelectron. J.* **2011**, *42*, 1400.
(35) Silaghi-Dumitrescu, I.; Lara-Ochoa, F.; Haiduc, I. *J. Mol. Struct.* **1996**, *370*, 17.
(36) Beheshtian, J.; Bagheri, Z.; Kamfiroozi, M.; Ahmadi, A. *J. Mol. Model.* **2012**, *18*, 2653.
(37) Saeedi, M.; Anafcheh, M.; Ghafouri, R.; Hadipour, N. L. *Struct. Chem.* **2012**, *24*, 681.
(38) Liu, Z. F.; Wang, X. Q.; Liu, G. B.; Zhou, P.; Sui, J.; Wang, X. F.; Zhuan, H. J.; Hou, Z. L. *Phys. Chem. Chem. Phys.* **2013**, *15*, 8186.
(39) Koi, N.; Oku, T.; Narita, I.; Suganuma, K. *Diamond. Relat. Mater.* **2005**, *14*, 1190.
(40) Oku, T.; Nishiwaki, A.; Narita, I. *Sci. Technol. Adv. Mater.* **2004**, *5*, 635.
(41) Yang, Z. H.; Shi, L.; Chen, L. Y.; Gu, Y. L.; Cai, P. J.; Zhao, A. W.; Qian, Y. T. *Chem. Phys. Lett.* **2005**, *405*, 229.
(42) Li, J. L.; Xia, Y. Y.; Zhao, M. W.; Liu, X. D.; Song, C.; Li, L. J.; Li, F.; Huang, B. D. *J. Phys.: Condens. Matter* **2007**, *19*, 346228.
(43) Zhang, D. J.; Zhang, R. Q. *J. Mater. Chem.* **2005**, *15*, 3034.
(44) Zope, R. R.; Dunlap, B. I. *Phys. Rev. B* **2005**, *72*, 045439.
(45) Wu, H. S.; Zhang, F. Q.; Xu, X. H.; Zhang, C. J.; Jiao, H. *J. Phys. Chem. A* **2003**, *107*, 204.
(46) Wang, Q.; Sun, Q.; Jena, P.; Kawazoe, Y. *ACS Nano* **2009**, *3*, 621.
(47) Zhang, Y. H.; Zheng, X. Z.; Zhang, S. L.; Huang, S. P.; Wang, P.; Tian, H. P. *Int. J. Hydrogen. Energy* **2012**, *37*, 12411.
(48) Beheshtian, J.; Peyghan, A. A.; Bagheri, Z. *Comput. Mater. Sci.* **2012**, *62*, 71.
(49) Beheshtian, J.; Peyghan, A. A.; Bagheri, Z. *Appl. Surf. Sci.* **2012**, *259*, 631.
(50) Zhang, C. Y.; Cui, L. Y.; Wang, B. Q.; Zhang, J.; Lu, J. *J. Struct. Chem.* **2012**, *53*, 1031.
(51) Rabilloud, F. *J. Phys. Chem. A* **2010**, *114*, 7241.
(52) Chandrakumar, K. R. S.; Ghosh, S. K. *Nano Lett.* **2008**, *8*, 13.
(53) Sun, Q.; Jena, P.; Wang, Q.; Marquez, M. *J. Am. Chem. Soc.* **2006**, *128*, 9741.
(54) Wang, Q.; Jena, P. *J. Phys. Chem. Lett.* **2012**, *3*, 1084.
(55) Li, Y. C.; Zhou, G.; Li, J.; Gu, B. L.; Duan, W. H. *J. Phys. Chem. C* **2008**, *112*, 19268.
(56) Wu, G. F.; Wang, J. L.; Zhang, X. Y.; Zhu, Li. Y. *J. Phys. Chem. C* **2009**, *113*, 7052.
(57) Venkataramanan, N. S.; Belosludov, R. V.; Note, R.; Sahara, R.; Mizuseki, H.; Kawazoe, Y. *Chem. Phys.* **2010**, *377*, 54.
(58) Xu, H. L.; Zhang, C. C.; Sun, S. L.; Su, Z. M. *Organometallics* **2012**, *31*, 4409.
(59) Karamanis, P.; Pouchan, C. *J. Phys. Chem. C* **2012**, *116*, 11808.
(60) Xu, H. L.; Li, Z. R.; Wu, D.; Ma, F.; Li, Z. J.; Gu, F. L. *J. Phys. Chem. C* **2009**, *113*, 4984.
(61) Ma, F.; Zhou, Z. J.; Li, Z. R.; Wu, D.; Li, Y.; Li, Z. S. *Chem. Phys. Lett.* **2010**, *488*, 182.
(62) Xu, H. L.; Zhong, R. L.; Sun, S. L.; Su, Z. M. *J. Phys. Chem. C* **2011**, *115*, 16340.
(63) Ma, F.; Zhou, Z. J.; Liu, Y. T. *Chem. Phys. Chem.* **2012**, *13*, 1307.
(64) Zhong, R. L.; Xu, H. L.; Sun, S. L.; Qiu, Y. Q.; Su, Z. M. *Chem.—Eur. J.* **2012**, *18*, 11350.
(65) Buckingham, A. D. *Adv. Chem. Phys.* **1967**, *12*, 107.
(66) Mclean, A. D.; Yoshimine, M. *J. Chem. Phys.* **1967**, *47*, 1927.
(67) Frisch, M. J.; Trucks, G. W.; Schlegel, H. B.; Scuseria, G. E.; Robb, M. A.; Cheeseman, J. R.; Montgomery, J. A., Jr.; Vreven, T.; Kudin, K. N.; Burant, J. C.; Millam, J. M.; Iyengar, S. S.; Tomasi, J.; Barone, V.; Mennucci,B.; Cossi,M.; Scalmani,G.; Rega, N.; Petersson, G. A.; Nakatsuji, H.; Hada, M.; Ehara, M.; Toyota, K.; Fukuda, R.; Hasegawa, J.; Ishida, M.; Nakajima, T.; Honda, Y.; Kitao, O.; Nakai, H.; Klene, M.; Li, X.; Knox, J. E.; Hratchian, H. P.; Cross, J. B.; Bakken, V.; Adamo, C.; Jaramillo, J.; Gomperts, R.; Stratmann, R. E.; Yazyev, O.; Austin, A. J.; Cammi, R.; Pomelli, C.; Ochterski, J. W.; Ayala, P. Y.; Morokuma, K.; Voth, G. A.; Salvador, P.; Dannenberg, J. J.; Zakrzewski, V. G.; Dapprich, S.; Daniels, A. D.; Strain, M. C.; Farkas, O.; Malick, D. K.; Rabuck, A. D.; Raghavachari, K.; Foresman, J. B.; Ortiz, J. V.; Cui, Q.; Baboul, A. G.; Clifford, S.; Cioslowski, J.; Stefanov, B. B.; Liu, G.; Liashenko, A.; Piskorz, P.; Komaromi, I.; Martin, R. L.; Fox, D. J.; Keith, T.; AlLaham, M. A.; Peng, C. Y.; Nanayakkara, A.; Challacombe, M.; Gill,P. M. W.; Johnson, B.; Chen, W.; Wong, M. W.; Gonzalez, C.; Pople, J. A. *Gaussian 09*, Revision A02; Gaussian, Inc.: Wallingford, CT, 2009.
(68) Oudar, J. L. *J. Chem. Phys.* **1977**, *67*, 446.
(69) Kanis, D. R.; Ratner, M. A.; Marks, T. *J. Chem. Rev.* **1994**, *94*, 195.
(70) Chen, W.; Yu, G. T.; Jin, P.; Li, Z. R.; Huang, X. R. *J. Comput. Theor. Nanosci.* **2011**, *8*, 2482.
(71) Li, Z. J.; Wang, F. F.; Li, Z. R.; Xu, H. L.; Huang, X. R.; Wu, D.; Chen, W.; Yu, G. T.; Gu, F. L.; Aokib, Y. *Phys. Chem. Chem. Phys.* **2009**, *11*, 402.